THE BELL SYSTEM TECHNICAL JOURNAL
Vol. 61, No. 9, November 1982
Printed in U.S.A.

A Description of the Bell Laboratories Scanned Acoustic Microscope

By P. SULEWSKI,* D. J. BISHOP, and R. C. DYNES

(Manuscript received February 4, 1982)

We have developed a working scanning reflection acoustic microscope. In this paper we describe its construction and operation and also present preliminary acoustic micrographs and compare them with equivalent optical and electron micrographs. Our instrument operates at room temperature using 2-GHz acoustic radiation with water as a coupling medium, and has a resolution of approximately 1 μm. We also discuss improvements to be made in future instruments with liquid helium as a coupling medium.

I. INTRODUCTION

Scanning reflection acoustic microscopy uses the amplitude of reflected high-frequency sound waves as a contrast mechanism to generate micrographs with submicrometer resolution. This method was first reported in 1974 by R. A. Lemons and C. F. Quate.[1] Since that time, much progress has been made in the field, including a steady improvement in the resolution of the instrument.[2] To date, acoustic microscopy has been used to study integrated circuits, biological specimens, and various materials with much success.[2]

Although acoustic micrographs appear quite similar to their optical counterparts, the source of the acoustic contrast lies in the mechanical properties of the sample. Hence, acoustic micrographs provide information that is fundamentally different from that of optical micrographs. Since the acoustic reflectivity at a surface is a strong function of the layering structure beneath,[3] much effort has been directed toward nondestructive analysis and characterization of integrated circuit defects using acoustic microscopy. In our research, it is hoped that variations in stress and crystal orientation near dislocations in crystals

* Princeton University.

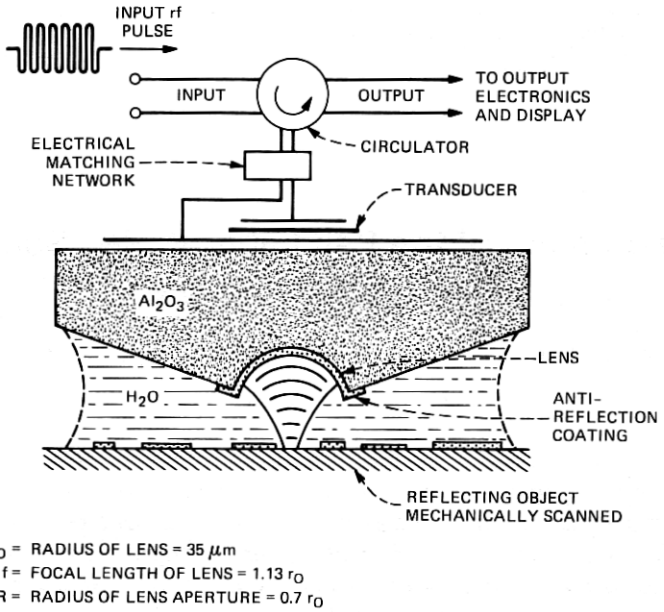

Fig. 1—The lens configuration of the scanning acoustic microscope.

will provide sufficient acoustic contrast to image dislocations, providing a powerful tool for nondestructive analysis.

Here we present micrographs from some preliminary surface studies, indicating the performance of our acoustic microscope, along with an explanation of its basic operation and components.

II. PRINCIPLES OF OPERATION

Our micrographs are generated using the acoustic lens pictured in Fig. 1. While using such a simple lens optically would result in severe distortion owing to spherical aberration, such effects are negligible in the acoustic case, since the distortion is proportional to the square of the ratio of the velocity of sound in the two media, sapphire and water. Since $V_{Al_2O_3} = 11.1$ km/s and $V_{H_2O} = 1.5$ km/s, such aberration effects can be ignored.[1] A coupling medium, in our case water, is used since air cannot transmit 2-GHz acoustic waves with acceptable losses.

The lens focuses the acoustic waves to a point, whose actual width is diffraction limited to of the order of λ. With the sample at this focal point, the acoustic waves are reflected back through the lens. The amplitude of the reflected waves provides the contrast for each resolution element in the final picture. Light and dark areas arise from variations in the acoustic reflectivity of the sample. Since the focal

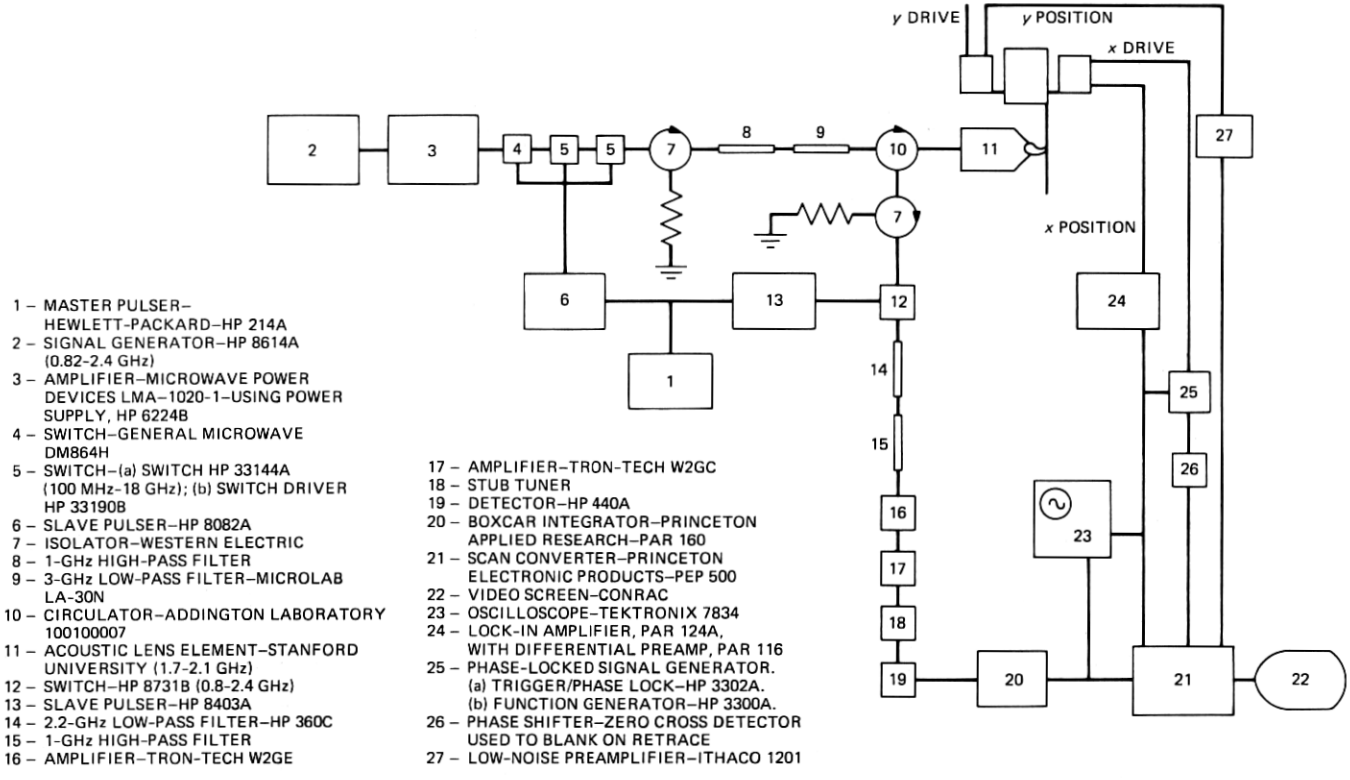

Fig. 2—Block diagram of the electronics for the microscope.

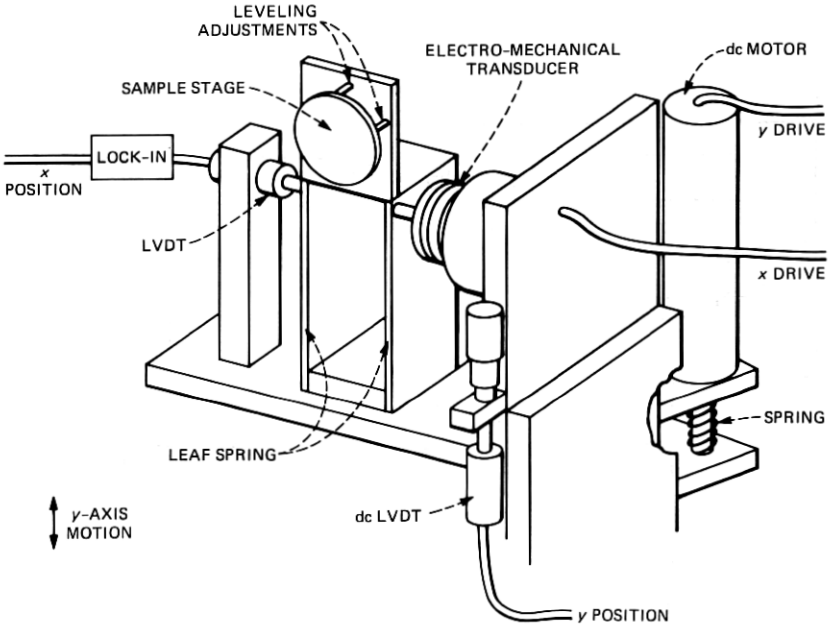

Fig. 3—The mechanical stage for the scanning acoustic microscope.

point has finite width, the resolution of the resulting micrograph is limited to $\approx 0.75\lambda$, as calculated by Wickramasinghe.[4]

To create a picture, the sample is scanned in a raster pattern, line by line. This is accomplished by vibrating the sample at a frequency of 37 Hz and an amplitude of ± 250 μm in the x direction, while driving the sample through 500 μm in the y direction in 10 to 15 seconds, completely scanning the sample. The amplitude of the reflected acoustic wave is then used together with x and y positioning information given by linear variable differential transformers (LVDT) to create a video image by a scan converter.

The acoustic waves are generated by a piezoelectric transducer on the back of the lens element, which converts microwaves at a frequency near 2 GHz to acoustic waves of the same frequency.

A master pulser, (1) in Fig. 2, governs the timing of the electronics that control and process the microwave power. The master pulser generates trigger pulses at a rate of 500 kHz. The microwaves are generated (2) and then amplified (3) to a power level of 1 watt. Three PIN-diode switches (4, 5) connected in series chop the continuous waves into 18-ns pulses at a rate set by the master pulser. An intermediate slave pulser (6) drives the switches. The use of pulsed waves allows us to isolate the desired information pulse from spurious reflec-

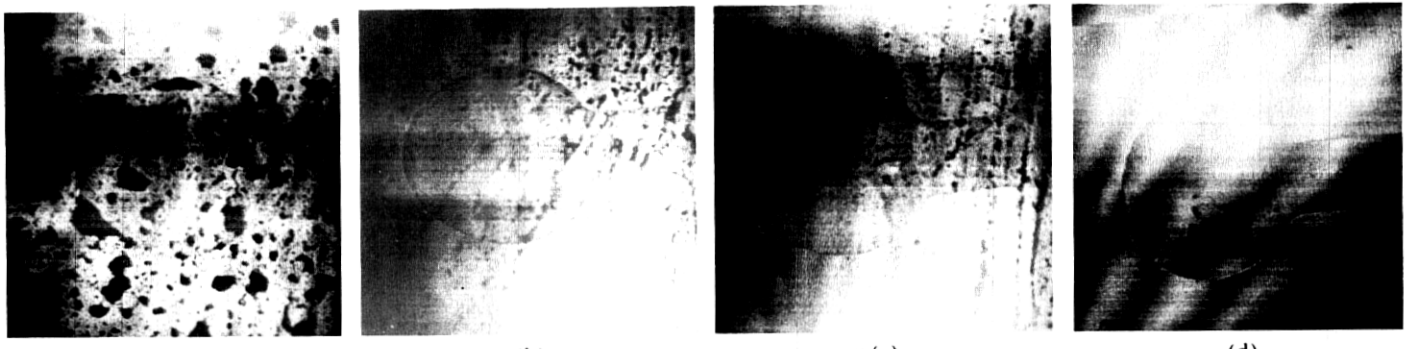

(a) (b) (c) (d)

Fig. 4—Acoustic micrograph of gold mask on epitaxially grown LED (layers of InP, InGaAsP,InP). (a) Before cleaning. (b) After swabbing with cotton swab soaked in ethanol. (c) After swabbing with alcohol. (d) With lens off focus slightly (or at different focus).

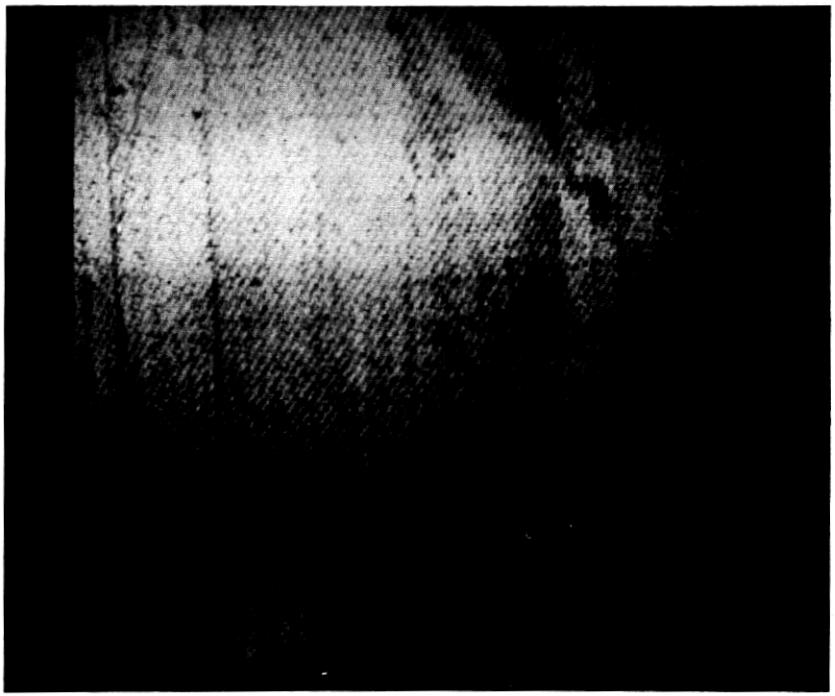

Fig. 5—Gold stripes on silicon.

tions. Three switches are used in series to increase the on-off ratio. Since the power of the desired reflected signal pulse is generally 80 dB below that of the initial pulse, any leakage of microwaves during the off state would produce undesirable interference patterns.

The microwave pulse then passes through an isolator (7) which protects the system from spurious multiple reflections. A 1-GHz high-pass filter (8) and a 3-GHz low-pass filter (9) eliminate low-frequency and high-frequency noise, respectively, from the switches. A circulator (10) directs the pulse into the lens element (11), and then directs the reflected signal pulse into the rest of the circuit.

At the back of the lens, the pulse is electrically matched to the piezoelectric transducer as in Fig. 1. Even with this matching network, there is a large reflection at this point. The transducer, composed of a gold-ZnO_2-gold sandwich, evaporated onto the back of the sapphire, converts the microwave pulse into an acoustic pulse of the same frequency, which then travels through the sapphire to the lens. At a simple lens-water interface, most of the incident radiation would be reflected since there is a large impedance mismatch, as $Z_{H_2O} = 1.5 \times 10^5 gm/cm^2\text{-}s$ and $Z_{Al_2O_3} = 44.0 \times 10^5 gm/cm^2\text{-}s$. A one-quarter-wavelength impedance-matching layer of borosilicate glass at this interface

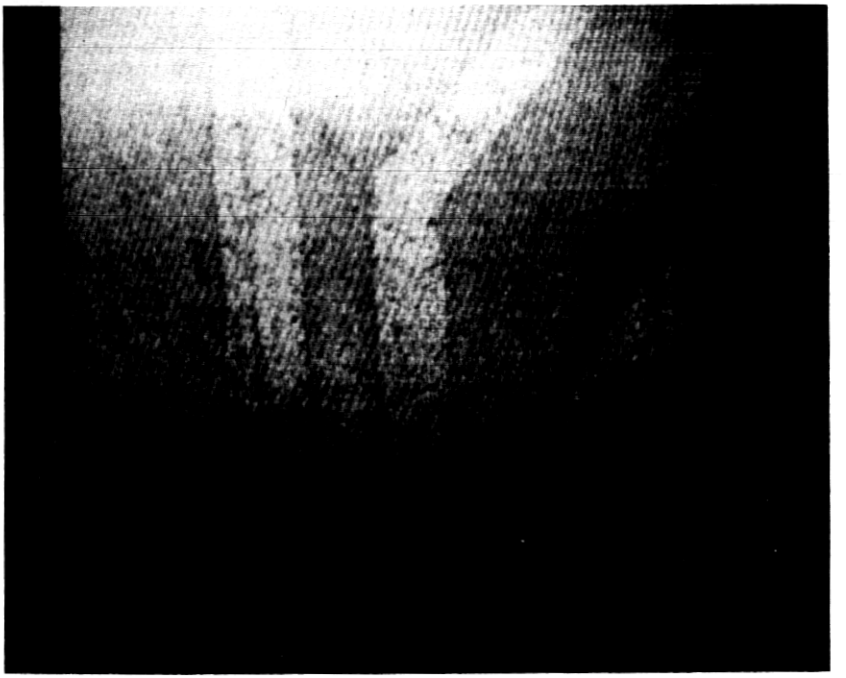

Fig. 6—A different region of gold stripes on silicon pattern shown in Fig. 5.

significantly increases transmission although it does not completely eliminate this reflection.[5] The transmitted and focused acoustic pulse then reflects off of the sample and back through the lens to the transducer, where it is reconverted into microwaves. Losses in the water amount to ≈70 dB. The amplitude of the reflected pulse depends upon the acoustic properties of the sample; hence, the contrast in the resulting micrograph reflects variations in acoustic properties of the sample. The pulse passes through an isolator (7) and a final PIN-diode switch (12), which acts as a window to protect the amplifiers from the large spurious reflections already mentioned. Two filters (14, 15) reduce the noise, especially low frequencies from the switch. The amplifiers (16, 17) give a total of 62-dB amplification. A stub tuner (18) matches the incoming transmission line to the crystal-diode detector (19). The detector rectifies the pulse of microwaves, and a boxcar integrator (20) is used to improve the signal-to-noise ratio. The scan converter (21) uses the x and y positioning information together with the signal pulse amplitude to construct a video picture, which may then be photographed from the screen (22).

The scan electronics provide the means to scan the sample in a

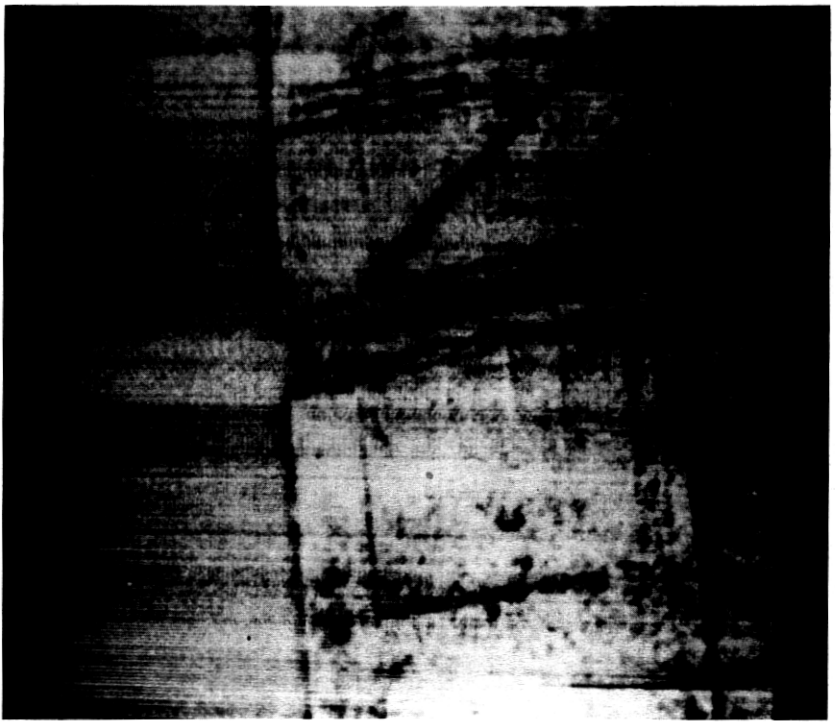

Fig. 7—Gold stripes with scratches on silicon.

raster pattern. The resolution of the LVDTs used must be submicrometer if the resolution in the microscope itself is to be submicrometer.

The sample stage (shown in Fig. 3) is mounted on leaf springs so that vibration of the sample is possible only in the x direction. The frequency of this vibration is held at resonance, approximately 37 Hz, using a phase-locked signal generator (25). Translation in the y direction is accomplished by an optical translation stage driven by a dc motor. Most of the weight of the stage is supported by a spring to relieve the motor, so that it can be operated without stalling.

The x positon of the sample is given by an ac LVDT connected to a lock-in amplifier (24). The y position is given by a dc LVDT whose output voltage is proportional to the displacement. It was found that the 10-kHz modulation frequency used to operate the LVDTs leaked into both x and y position signals, causing image degradation and poor resolution. Filtering these signals resulted in much improved images.

Since the theoretical resolution is proportional to λ, increasing the frequency should improve the resolution. However, for water and many other liquids, the acoustic attenuation is proportional to f^2, so

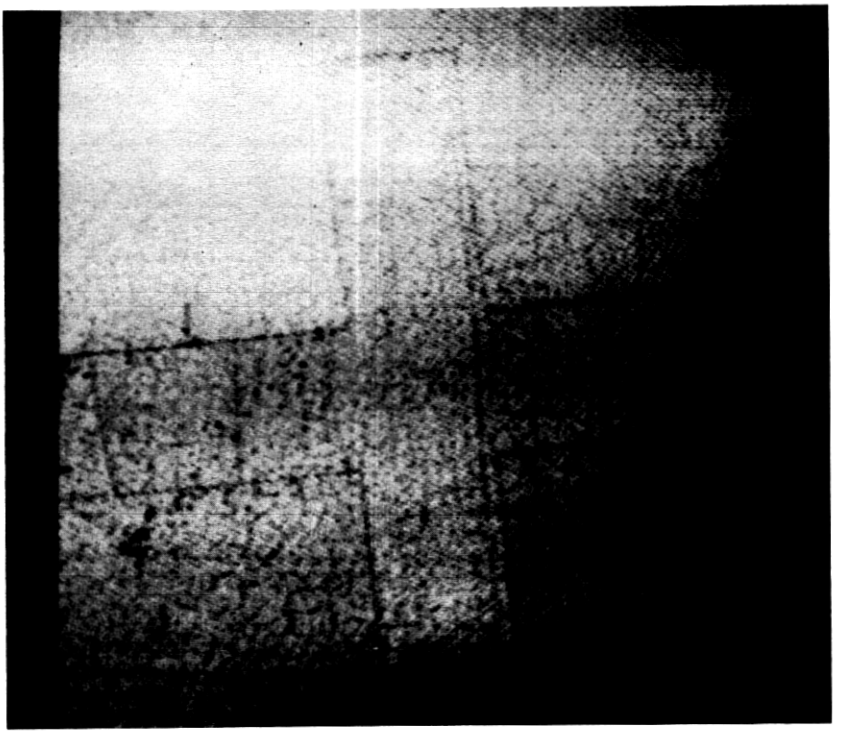

Fig. 8—Gold cross on silicon.

increasing the frequency dramatically increases the power losses within the coupling medium.[5] To preserve the signal-to-noise ratio, 1.8 to 2.0 GHz is the present optimal frequency range. Other coupling media continue to be investigated.

We use water heated to 60°C, where the acoustic attenuation is lower than at room temperature, resulting in an improved signal-to-noise ratio.

We have found that both samples and lens must be kept very clean if the microscope is to function at all. A very thin film of oil, like that deposited by a fingerprint, can reduce the amplitude of the reflected pulse dramatically. Also any small dust particle, with a diameter of several micrometers, which becomes lodged in the lens will distort and even eliminate the reflected signal pulse.

III. IMAGES

For our initial testing of the microscope, various surface structures were examined, and comparisons performed with optical and electron micrographs.

Fig. 9—Bulk-epitaxial transition InGaAsP; left, bulk; right, epitaxial.

The first series of micrographs in Fig. 4 of a gold mask on InGaAsP indicates the importance of surface cleaning. Any oil or grease, for example a fingerprint or any of the vacuum grease used to fix the sample to the stage, shows up quite clearly and obscures the true detail (Fig. 4a). Cleaning the surface with a cotton swab soaked in ethanol significantly reduces the surface structure of the first micrograph (Fig. 4b,c). Fig. 4d presents another method of discerning true structure from mere surface dirt effects. By maintaining the lens slightly out of focus, the effects of surface dirt disappear. Also note the phase shifts at the edges of the gold to InGaAsP transition owing to different acoustic path lengths in the materials. The diagonal lines visible in Fig. 5, 6, and 7 are caused by noise over the signals given by the LVDTs. This effect was eliminated from subsequent micrographs. The noise produced an uncertainty of several micrometers in the sample position, seriously degrading image resolution.

Fig. 8 displays the dramatic improvement in image quality achieved by eliminating the noise over the LVDT signals. The horizontal dark and light bands result when the dc motor alternately slows down or speeds up within the single frame. Near the bottom of the picture,

(a) (b) (c)

Fig. 10—Indium inclusion in epitaxial InGaAsP. (a) Optical micrograph. (b) Electron micrograph. (c) Acoustic micrograph.

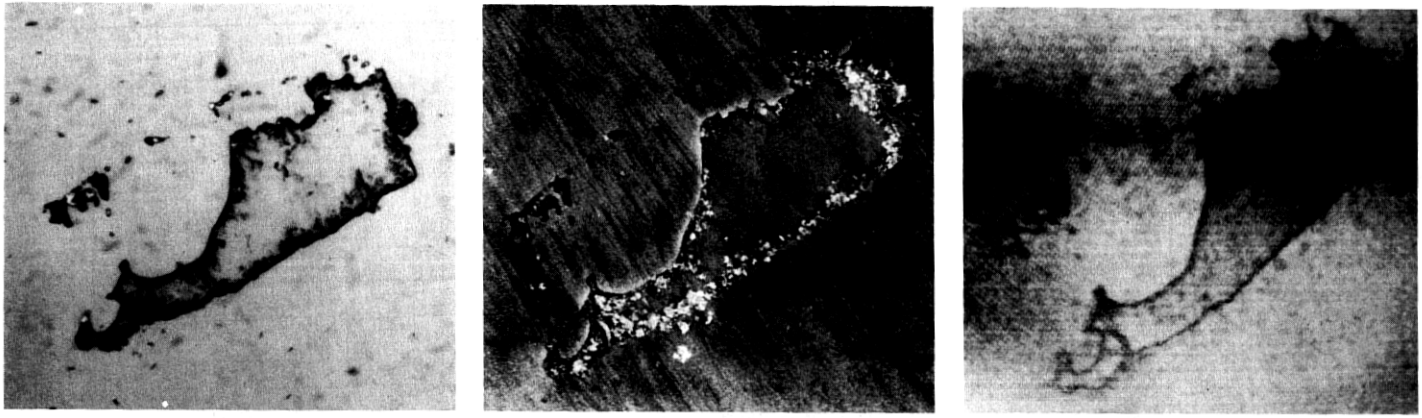

(a) (b) (c)

Fig. 11—Indium inclusion on epitaxial layer. (a) Optical. (b) Electron. (c) Acoustic.

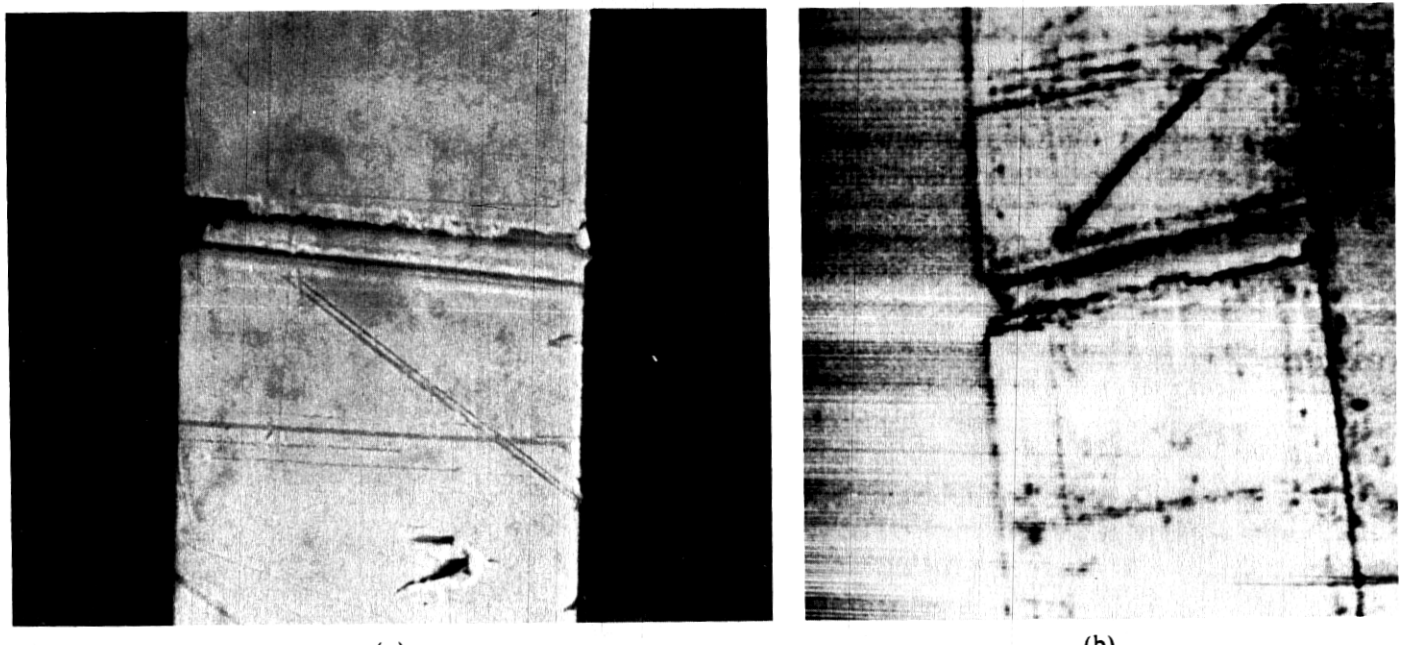

(a) (b)

Fig. 12—Gold stripe on silicon. (a) Electron. (b) Acoustic.

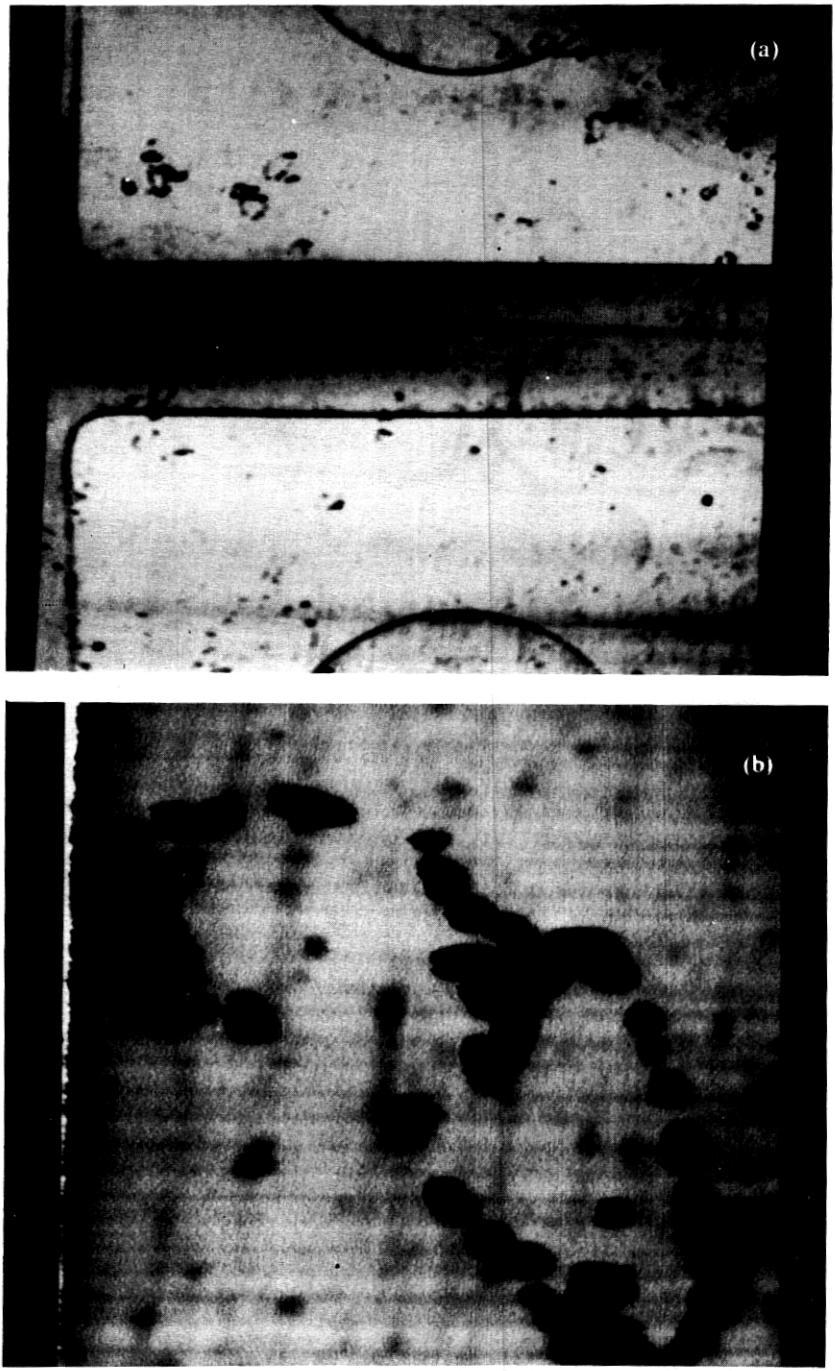

Fig. 13—(a) A sample of InGaAsP is shown with a gold evaporation on the surface. The dark regions are indium inclusions which have formed on the surface. The field of view is ≈500 μm × 500 μm. (b) A close-up of an inclusion from Fig. 13a at ten times the magnification.

Fig. 14—A more recent micrograph of gold on silicon showing the quality of the acoustic micrographs we have been able to obtain.

single scan lines are visible. This problem has been overcome with a better mechanical drive.

One area of application of the acoustic microscope is the evaluation of subsurface defects within epitaxial layers. Preliminary to such studies, we have examined various samples of epitaxially grown wafers with inclusions visible on the surface. The first picture in the series, Fig. 9, shows a transition from bulk to epitaxial InGaAsP, from left to right.

In Fig. 10, we compare optical, electron, and acoustic micrographs of an indium inclusion in an epitaxial layer of InGaAsP. In the acoustic picture, in the lower right opening in the inclusion, several round spots a few micrometers across appear, which do not appear in either the electron or optical micrographs. These could be subsurface features that only the acoustic microscope can image.

The next series of pictures in Fig. 11 show another indium inclusion on the same sample. Again while more surface features are visible with optical and electron microscopy, there is a round spot 5 μm in diameter near the lower edge of the inclusion in the acoustic micrograph that does not appear in either of the other pictures.

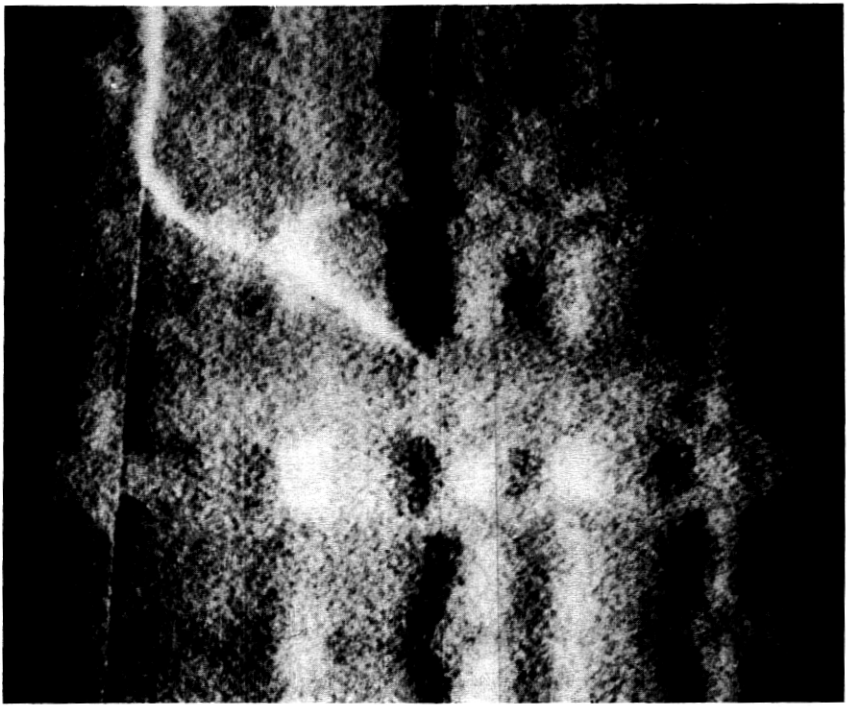

Fig. 15—This micrograph shows an image where the derivative of the acoustic intensity is plotted. This type of photo provides a sense of depth perception to the photos and generates a microscopic contour map.

In Fig. 12, we present a comparison between electron and acoustic micrographs of a 50-μm gold strip evaporated onto silicon. The scratch marks provide a good measure of the resolution of the instrument. The top two horizontal scratches are 5 μm apart, and easily discerned in the acoustic micrograph. The bottom three scratches are each 2.5 μm apart from the other and also easily discernible. However, the two diagonal scratches, separated by 1 μm, are not distinguishable in this micrograph.

In Fig. 13, we show a recent micrograph of an InGaAsP sample with a gold overlayer. The instrument has been optimized for this series of pictures and gives some indications of the quality that it is capable of. The small dark regions are indium inclusions which have formed on top of the sample. Figure 13b, is a micrograph of a single inclusion seen in the center of the upper photo.

In Fig. 14, we show a picture of gold stripes evaporated on a silicon substrate. Finally in Fig. 15, we show the results of a form of derivative microscopy. In that picture, we have displayed the derivative of the

acoustic amplitude. This produces an image which is a micro-contour map of the substrate.

IV. CONCLUSIONS

We have successfully operated a scanning acoustic microscope at 60°C with resolution approaching the diffraction limit using water as a transmitting medium. Our instrument operates at 1.9 GHz with a resolution of ≈ 1 μm. We have shown some preliminary acoustic micrographs indicating how our present instrument might be used in studies of structural defects in various materials of technological importance.

Work is currently under way to develop an instrument using liquid He^4 as an acoustic transmitting medium, which will allow us to use much higher acoustic frequencies. Such a device will be the first acoustic microscope that will not have diffraction-limited resolution.

ACKNOWLEDGMENTS

We wish to thank R. A. Lemons, J. E. Heiserman, C. F. Quate, A. K. Chin, and A. Atalar for useful discussion. In addition we would like to thank C. F. Quate for providing the acoustic lens used in these studies.

REFERENCES

1. R. A. Lemons and C. F. Quate, "Acoustic Microscope—Scanning Version," Appl. Phys. Lett., *24*, No. 4 (February 1974), pp. 163–5.
2. See for example R. A. Lemons and C. F. Quate, "Acoustic Microscopy," Physical Acoustics, *14*, R. N. Thurston (Editor), Academic Press (to be published).
3. A. Atlar, "An Angular-Spectrum Approach to Contrast in Reflection Acoustic Microscopy," J. Appl. Phys., *49*, No. 10 (October 1978), pp. 5130–9.
4. H. K. Wickramasinghe, "Contrast and Imaging Performance in the Scanning Acoustic Microscope," J. Appl. Phys., *50*, No. 2 (February 1979), pp. 664–72.
5. R. A. Lemons, *Acoustic Microscopy by Mechanical Scanning*, Ph.D. dissertation, Stanford University, 1975.